

MEASURED SPATIAL VARIABILITY OF BEACH EROSION DUE TO AEOLIAN PROCESSES.

Sierd de Vries¹, Anne Verheijen¹, Bas Hoonhout^{1,2}, Sander Vos¹, Nick Cohn³ and Peter Ruggiero³

Abstract

This paper shows the first results of measured spatial variability of beach erosion due to aeolian processes during the recently conducted SEDEX² field experiment at Long Beach, Washington, U.S.A.. Beach erosion and sedimentation were derived using series of detailed terrestrial LIDAR measurements of beach morphology during three low tide periods. Results show significant measured sedimentation and erosion up to 10-20 mm/hour during moderate wind conditions. Spatial variability in bed level changes were found which appeared to be related to the wind orientation and varying bed level characteristics. Around the high waterline, erosion is found during onshore winds whereas sedimentation is observed on the upper beach. The terrestrial lidar data also resolves the migration of bed forms migrating on the upper beach demonstrating its utility of for a range of aeolian sediment transport applications.

Key words: Aeolian sediment transport, terrestrial laser scanning, beach morphodynamics, SEDEX².

1. Introduction

Aeolian sediment transport in the coastal zone determines the sediment input to coastal dunes. Instantaneous aeolian sediment transport rates are determined by a combination of the wind's capacity to transport sediment and the availability of sediment for transport. Several studies on aeolian sediment transport on beaches have indicated that sediment availability is often limited (e.g. Houser, 2009; Nickling et. al., 1990). This finding implies that the availability of sediment for aeolian sediment transport on those beaches largely controls sediment transport rates, when and where erosion of the beach may occur, and associated net sediment input to the dunes.

Recent studies by de Vries et. al. (2014) and Hoonhout and de Vries (2017) have provided evidence that spatiotemporal variability in sediment availability on nourished beaches can cause spatiotemporal variability in aeolian sediment transport rates. They measured aeolian sediment transport gradients over the beach that show relatively large positive gradients in the direction of the wind at the lower beach and intertidal zone. This pattern indicates relatively large and significant erosion in the intertidal zone and at the lower beach when compared to the upper beach, implying that sediment availability is higher in the intertidal zone. The observations that erosion in the intertidal and lower beach can be relatively large is an important step in revealing the mechanisms of sediment exchange between the marine and aeolian parts of the coastal profile. Moreover, it sheds new light what processes are responsible for the spatiotemporal variability of the sediment availability and associated aeolian sediment transport rates as input towards coastal dunes. The work by de Vries et. al. (2014) and Hoonhout and de Vries (2017) focused on nourished as opposed to natural beaches and lacked the spatiotemporal resolution to explore in detail the specific processes involved.

In this study, we follow up on the hypothesis that spatiotemporal variability of sediment availability for aeolian sediment transport is influenced by marine processes such as waves, tide and the associated marine sediment transport. To explore this hypothesis, high resolution data on the morphological changes caused by wind, waves and tides are essential. We have gathered such data in the framework of the Sandbar-

¹Department of Hydraulic Engineering, Faculty of Civil Engineering and Geosciences, Delft University of Technology, Delft, Netherlands. Sierd.deVries@tudelft.nl, A.H.Verheijen@tudelft.nl, S.E.Vos@tudelft.nl

²Unit of Hydraulic Engineering, Deltares, Delft, Netherlands. bas.hoonhout@deltares.nl.

³College of Earth, Ocean and Atmospheric Sciences, Oregon State University, Corvallis, OR, 97331, USA.

pruggier@coas.oregonstate.edu, cohn@geo.oregonstate.edu

aEolian-Dune EXchange Experiment (SEDEX²) field campaign that was conducted at the Long Beach Peninsula in Washington (USA) in summer 2016 (Cohn et al., this volume). During this field campaign, we have developed a new method to measure sedimentation and erosion using spatially dense and frequently collected terrestrial laser scanner data.

2. Methodology

The field site for this study is Oysterville Beach located on the Long Beach Peninsula in Washington, U.S.A. (see Figure 1.). The Long Beach Peninsula is characterized by a high energy wave climate, low sloping beaches, and long-term progradation of the coastline (Ruggiero et al., 2005). The progradation rate of the coastline is 4 m/yr and observations show that the aeolian beach and dune system seems to follow the same rate of progradation (Ruggiero et al., 2016). This implies a significant sediment input in the dune system that is likely governed by aeolian processes but also influenced by the growth of vegetation as well as marine processes during high water level events. As the role of the sediment availability for aeolian sediment transport is yet to be determined at this site, detailed measurements of aeolian erosion at the beach will provide new insights.

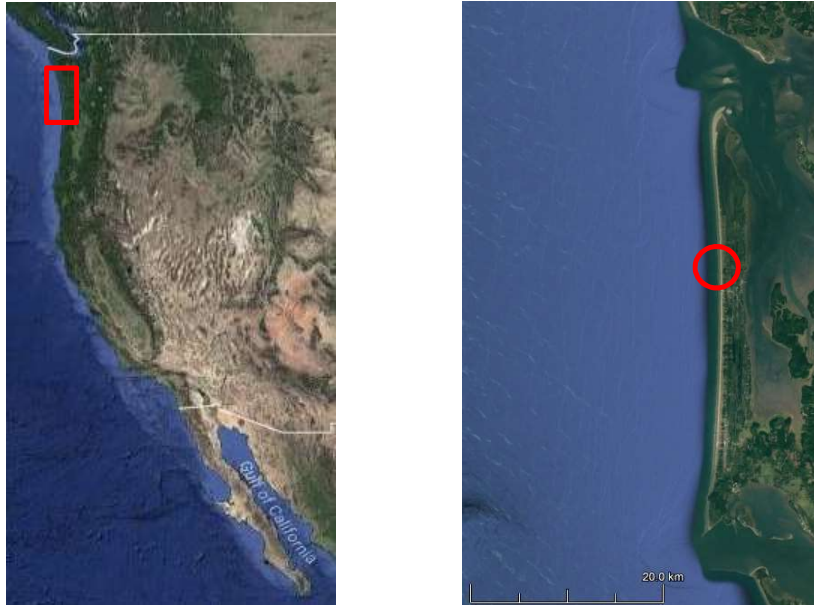


Figure 1. Field site location, Long Beach Washington, U.S.A.

To conduct detailed measurements of beach erosion and sedimentation we use a Riegl VZ2000 laser scanner in combination with new tailor made processing techniques. The scanner was set to make a series of 3D topographic scans of the beach surface covering the dry beach and intertidal zones. The scanner was placed on a 3.5 m high tripod at the high tide mark. The range of the scanner was on the order of 100 m and included the upper part of the intertidal area, the dry beach and the foredune. For practical and accuracy related reasons, we focused on a 100 x 100 m area around the scanner for the analysis described herein. See Figure 2 for an illustration of the scanner setup and domain. Time series of the sand surface were made with an interval of 7.5-15 minutes during periods with significant winds. A series of scans covering several hours were then used to derive patterns of significant sedimentation and erosion.

Anticipating that erosion and sedimentation on such small timescales will lead to very small deformation of topography, extra effort was invested in the calibration of the scanner position and orientation. For every individual scan, the scanner position and orientation was calibrated using 16 ground control points (GCPs). This turned out to be needed to omit small variations in scanner location and orientation that likely occurred due to small instabilities of the tripod itself, thermal deformation of the tripod and/or the deformation of the sand surface on which the tripod was placed.

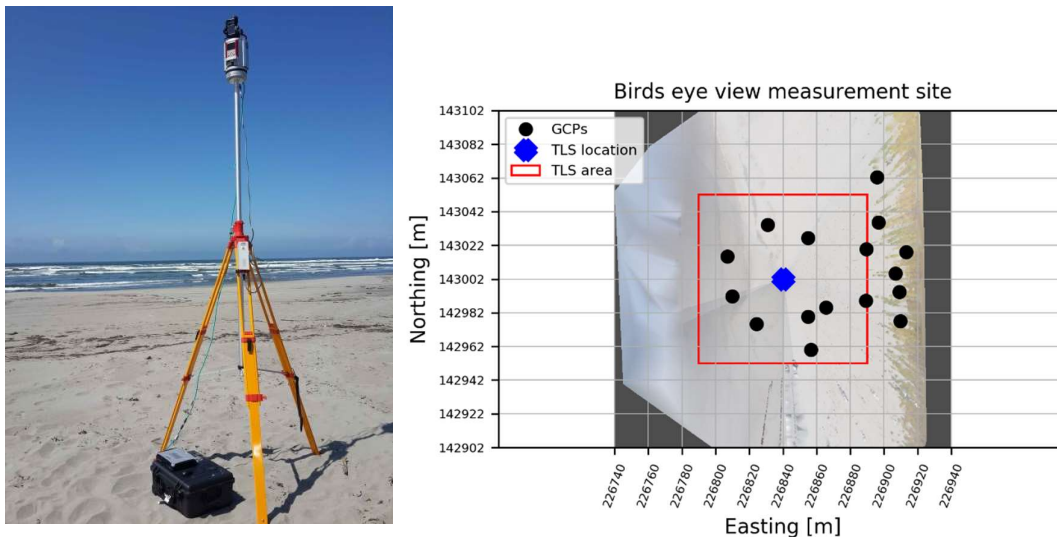


Figure 2, Laser scanner setup (left) and measurement domain indicating the scanner collation and ground control points(black circles, right). Note: the left side is the ocean side and the right side the dune side.

The processing of the scans consisted of 4 steps:

1. The scanner location and orientation of each individual scan was (re-)calibrated using ground control points. This step guarantees the best possible comparison between individual scans.
2. The obtained raw point clouds were filtered where reflectance values of less than -20dB were discarded as well as any points that were outside the physical range of the sand surface.
3. The vertical coordinates of the individual (filtered) point clouds in the series were each linearly interpolated on a horizontal grid covering a total area of 100 m by 100 m and grid cells with 0.03 m by 0.03 m resolution. This resolution was chosen based on the expected signature of the laser pulse (approximately 0.02 m) on the sand bed at a distance of 100 m from the scanner.
4. Time series of the vertical variability at each of the 11 million horizontal grid points were extracted from the grid and analyzed independently. For each grid point a linear curve was fitted through the time series. The fitting parameters of this linear curve (steepness, R^2) were used to derive and interpret erosion and sedimentation patterns. See figure 3 for an overview of the fitting procedure that is executed at every grid point.

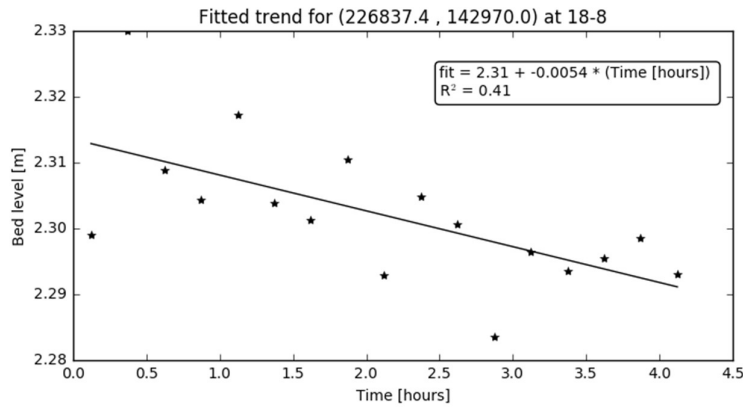


Figure 3. Example of fitted trend through bed level elevation. This example shows erosion of 5.4 mm/h with an R^2 of 0.41

3. Results

We have executed and analyzed for three time periods covering several hours each, totaling 73 scans as outlined in Table 1. Results consist of derived sedimentation and erosion patterns. All three measurement periods took place during low tide. Each of the scan periods is elaborated upon in the following subsections after which the similarities and differences are discussed.

Table 1. Details of SEDEX² terrestrial lidar scans

Date	High Tide Time (GMT)	Survey Start Time (GMT)	Survey End Time (GMT)	Avg. Wind Direction (°)	Avg. Wind Speed (m/s)	Number of Scans
18 August	21:18	22:47	2:47	314	7.1	17
29 August	19:24	20:47	0:47	182	6.6	32
30 August	20:12	22:50	1:50	153	6.8	24

3.1 August 18, 2016

The measuring sequence at August 18 started roughly 1 hour and 30 minutes after peak high tide and lasted for 4 hours. Every 15 minutes a scan was made resulting in 17 total scans that were used in the analysis for August 18. The average wind speed was 7.1 m/s from the northwest. Zones of erosion and sedimentation in the cross shore direction can be identified when analyzing the series of extracted cross shore transects in Figure 4. Erosion is particularly significant at the lower beach area (around $z = 2$ m) where measured transects later in time clearly show a lower bed level. Moving towards the upper beach, the calculated rates of erosion are lower. Zooming in near the high tide elevation, some spatial variability is visible that is likely related to the Lidar technique and its mounting. This variability is limited to several centimeters.

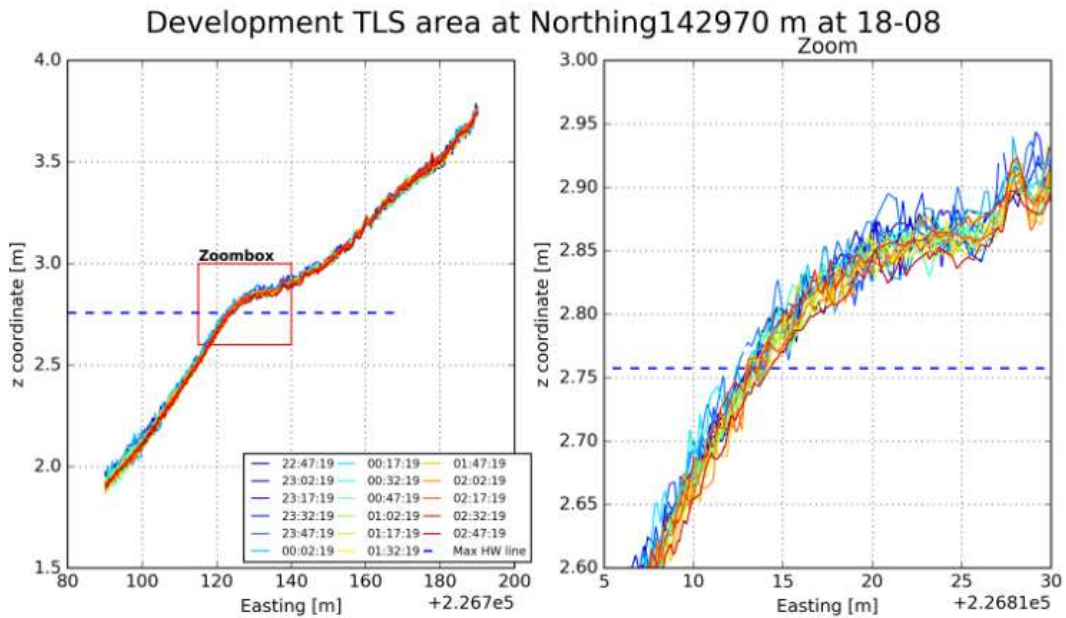


Figure 4, Left panel shows a time series of cross shore transects of bed level elevation on August 18th, 2016. The right panel shows a detail of the signal. See Figure 5 for the definition of the cross shore transect in the measurement domain.

The spatial representation of erosion and sedimentation based on the linear regression of the bed level in time at each grid point is shown in the top panel of Figure 5. The bottom panel of Figure 5 shows the associated R^2 values. It is shown that there is significant erosion at the lower beach/intertidal zone up to 20 mm/h. At the same time, sedimentation is visible at the upper beach of similar order. Strong local gradients are likely explained by migrating spatial features such as bed forms. Those features seem to be limited to the upper beach. The R^2 values show average values of around 0.4 but are significantly larger when rates of erosion/sedimentation are large such as at the locations of the migrating bed forms.

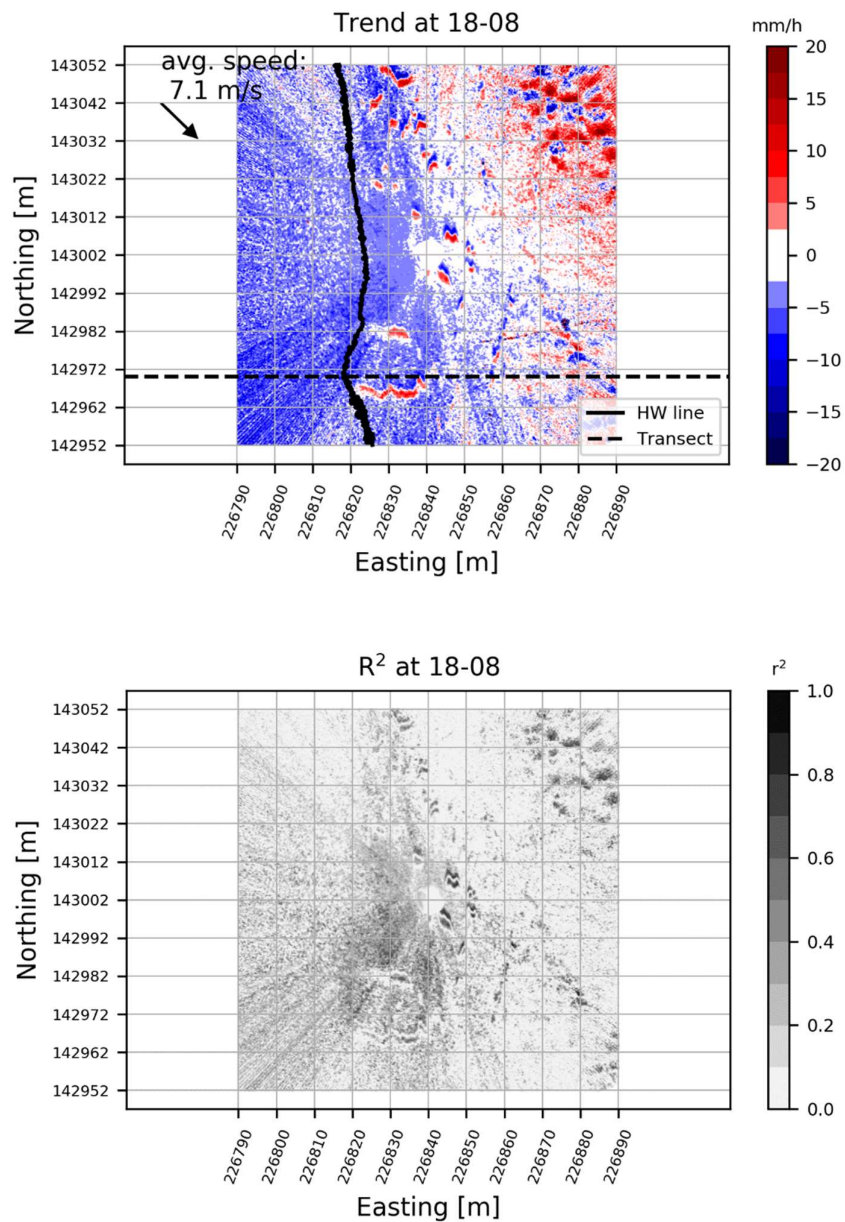


Figure 5 Top panel shows the spatial distribution of the fitted linear trend [mm/hours]. Bottom panel shows the associated R^2 of the fitted linear trend.

3.2 August 29, 2016

The measurement sequence on August 29 started roughly 1 hour and 30 minutes after high tide. During a period of 4 hours scans were made using a 7.5 minute interval resulting in a total number of 32 scans. The average wind speed was 6.6 m/s from the south. Zones of erosion and sedimentation in the cross-shore direction can be identified in Figure 6 where a series of cross-shore transects is plotted. Some erosion is visible just landward of the high water line. At the same time, spatial variability on the order of several centimeters is measured.

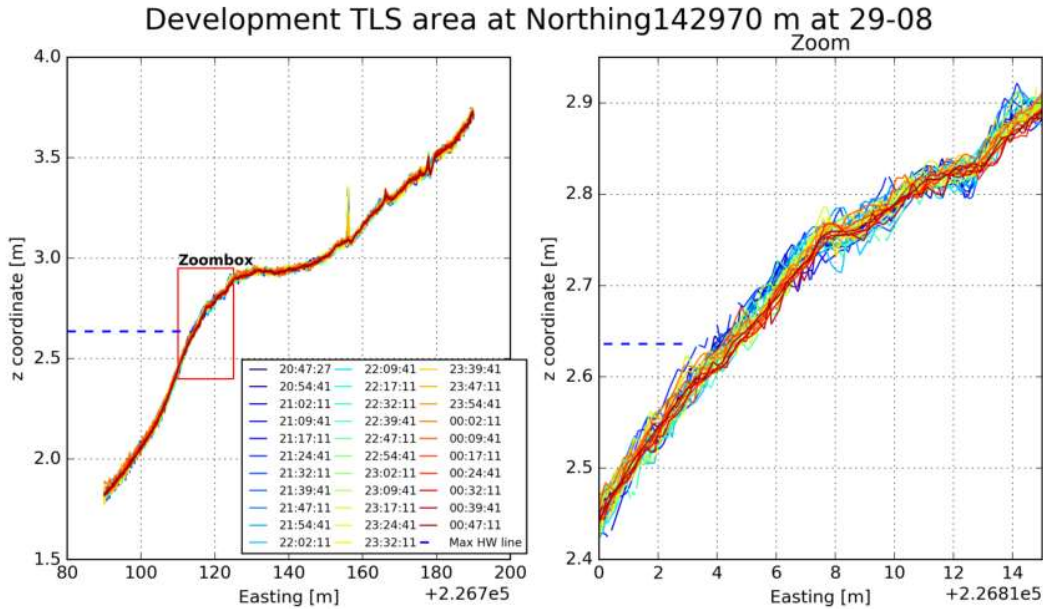


Figure 6. Left panel shows a time series of cross shore transects of bed level elevation on August 29th. The right panel shows a detail of the signal.

The spatial representation of erosion and sedimentation based on the linear regression of the bed level in time at each grid point is shown in the top panel of Figure 7. The bottom panel of Figure 7 shows the associated R^2 values. It is shown that sedimentation and erosion is limited, however there is significant erosion locally around the high water line in the order of 10-20 mm/h. On the upper beach strong local gradients are likely explained by migrating spatial features such as bed forms. The R^2 values show average values of around 0.4 where significant sedimentation and erosion is found.

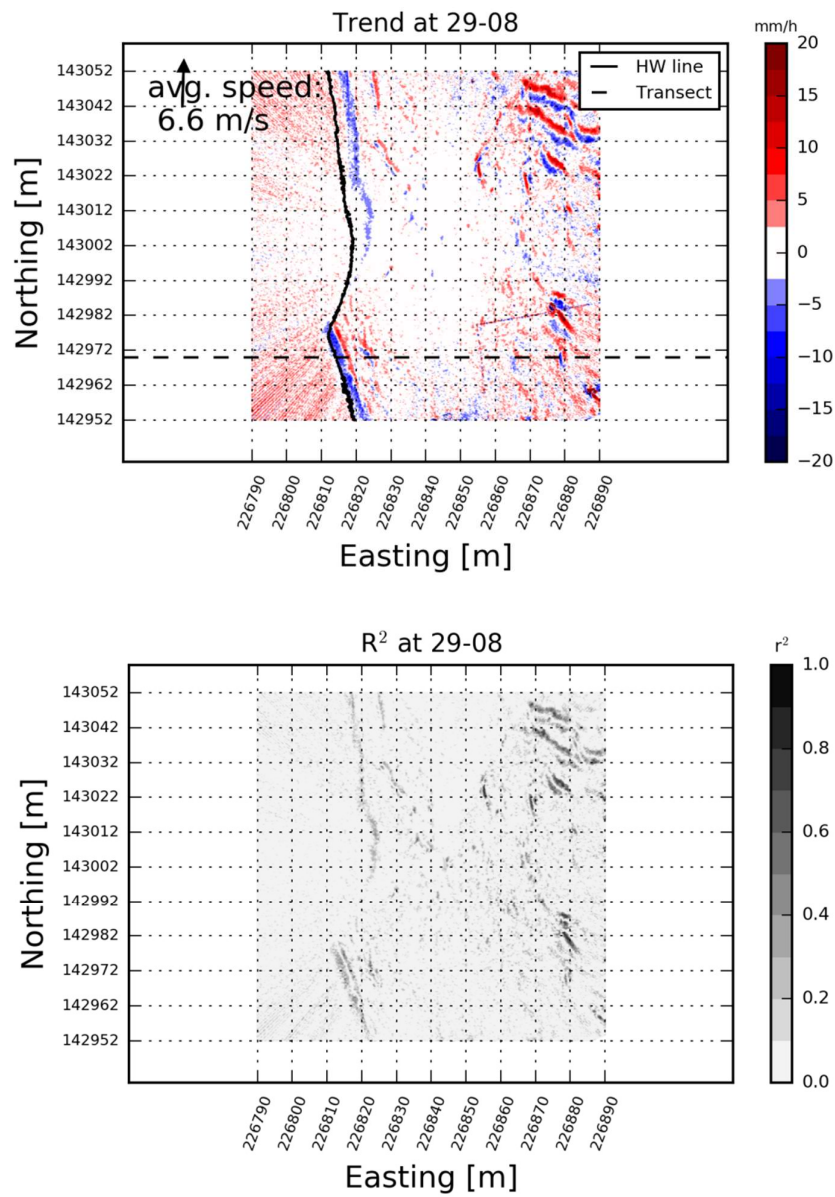


Figure 7. Top panel shows the spatial distribution of the fitted linear trend [mm/h] for scans on August 29. Bottom panel shows the associated R^2 of the fitted linear trend.

3.3 August 30, 2016

The measurement sequence on August 30 started roughly 2 hours and 30 minutes after the high tide. During a period of 3 hours scans were made using a 7.5 minute interval resulting in a total number of 24 scans. The average wind speed was 6.8 m/s from the south east. Zones of erosion and sedimentation in cross shore direction can be identified in Figure 8 where a series of cross shore transects is plotted. Some sedimentation and erosion is visible in the vicinity of the high water line. At the same time spatial variability in the order of several centimeters is measured.

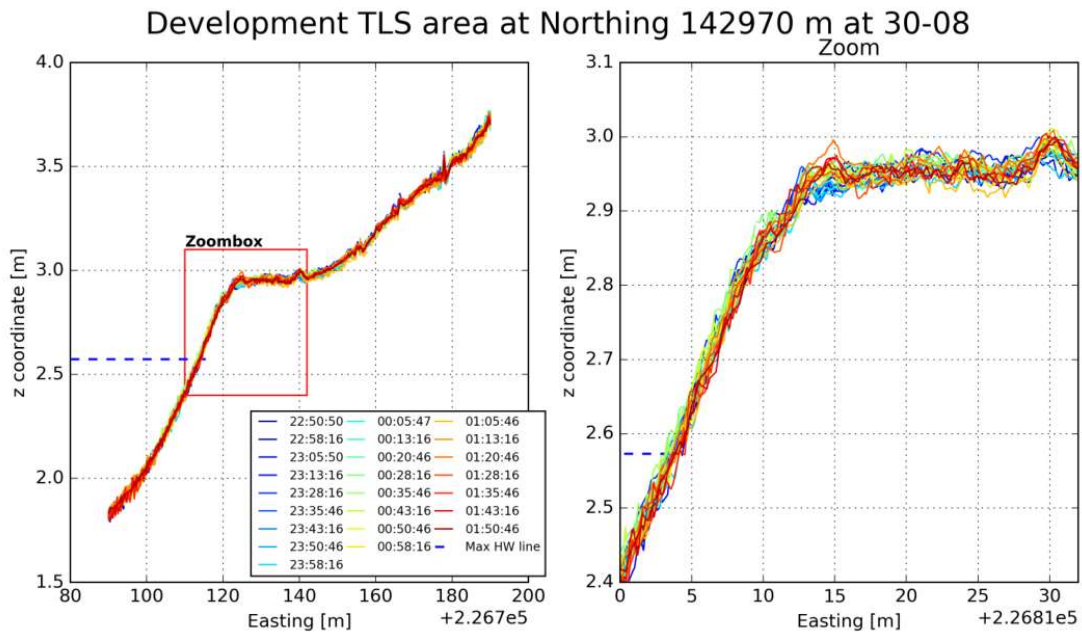


Figure 8. Left panel shows a time series of cross shore transects of bed level elevation on August 29th. The right panel shows a detail of the signal.

The spatial representation of erosion and sedimentation based on the linear regression of the bed level in time at each grid point is shown in the top panel of Figure 9. The bottom panel of Figure 9 shows the associated R^2 values. It is shown that sedimentation and erosion occurs at very specific locations. There is significant local sedimentation that seems to be organized in features both perpendicular as parallel to the wind direction. The local sedimentation is on the order of 10-20 mm/h. On the upper beach strong local gradients are likely explained by migrating spatial features such as bed forms. The R^2 values show average values of around 0.4 at the locations where significant sedimentation and erosion is found. Where sedimentation and erosion is small, the variability is relatively large and hence R^2 values are small.

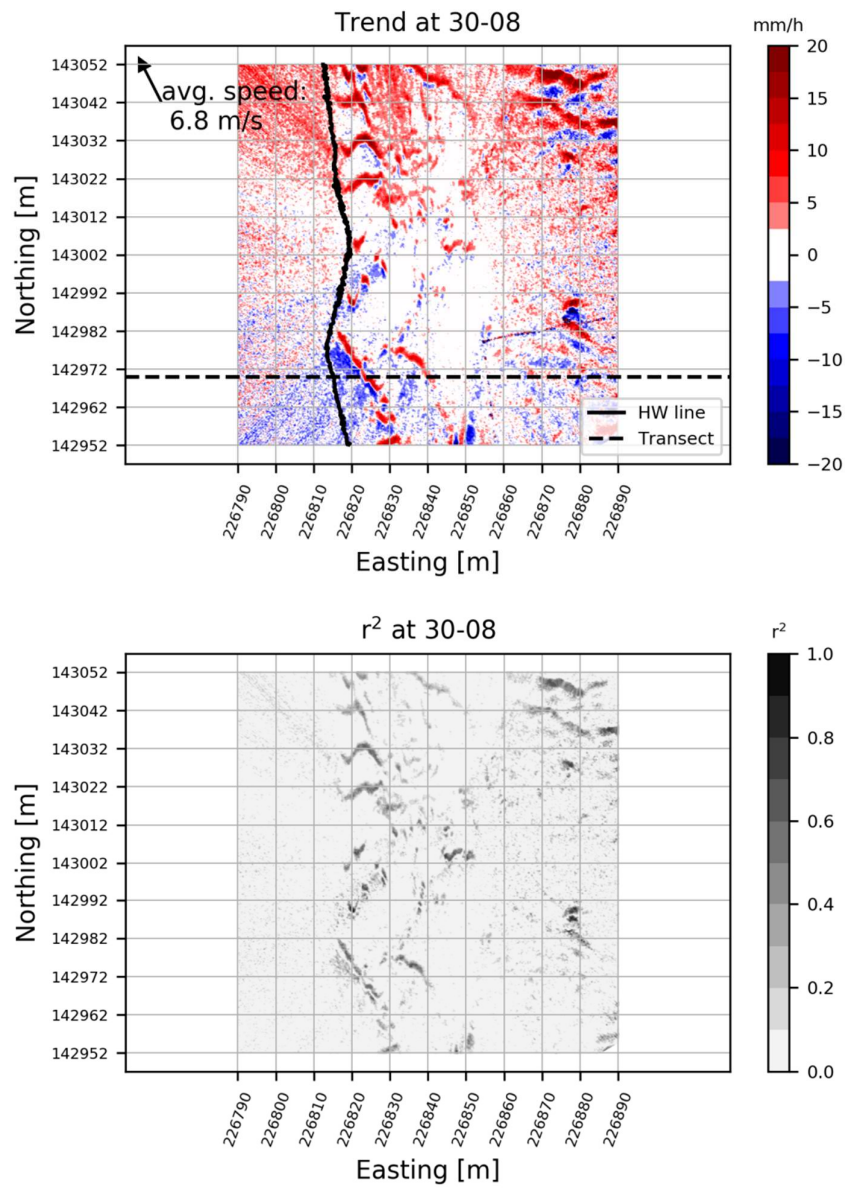


Figure 9. Top panel shows the spatial distribution of the fitted linear trend [mm/h] for scans on August 30. Bottom panel shows the associated R^2 of the fitted linear trend.

4. Conclusions

Variability of beach erosion due to aeolian sediment transport was derived based on measurements. Beach erosion and sedimentation were derived using series of detailed terrestrial LIDAR measurements of beach morphology during three low tide periods during the SEDEX² field campaign. Erosion and sedimentation up to 10-20 mm/h were derived.

The measurements suggest that sediment is relatively easily mobilized by aeolian processes in the vicinity of the high water line on the fine grained dissipative beach we studied. Despite the modest range of wind conditions and sub decimeter bed level changes occurring during the selected periods, clear patterns can be distinguished where erosion rates decrease in the direction of the upper beach.

The specific patterns of erosion near the high waterline might be explained by recent local (marine) deposits that positively influence sediment availability. However, it is unclear why exactly the erosion and sedimentation is confined to specific areas. Possible explanations for the lack of erosion at the upper beach include that negligible gradients in sediment transport might exist because the wind transport capacity was reached or sediment availability at the upper beach was limited. At the same time, seaward of the high water line, sediment availability might be limited by moisture content associated with the intertidal zone. In addition to that, the influence and importance of the measured migrating bedforms is unknown. In situ measurements during SEDEX² might provide additional insights on this.

References

- Cohn, N., Ruggiero, P., de Vries, S., and Garcia, G. (this volume). Beach growth driven by intertidal sandbar welding. *Proceedings of the Coastal Dynamics Conference 2017*
- de Vries, S., Arens, S.M., de Schipper, M.A., Ranasinghe, R., 2014 Aeolian sediment transport on a beach with a varying sediment supply, *Aeolian Research*, 15, 235-244.
- Hoonhout, B., De Vries, S., 2017. Field measurements on spatial variations in aeolian sediment availability at the Sand Motor mega nourishment, *Aeolian Research*, 24, 93-104.
- Houser, C., 2009. Synchronization of transport and supply in beach-dune interaction. *Progress in Physical Geography*, 33, 733-746
- Nickling, W., Davidson-Arnott, R., 1990. Aeolian sediment transport on beaches and coastal sand dunes. *Proceedings of the Symposium on Coastal Sand Dunes*, 1-35.
- Ruggiero, P., Kaminsky, G.M., Gelfenbaum, G., and Voigt, B., 2005. Seasonal to interannual morphodynamics along a high-energy dissipative littoral cell. *Journal of Coastal Research*, 21(3): 553-578.
- Ruggiero, P., Kaminsky, G. M., Gelfenbaum, G., Cohn, N., 2016. Morphodynamics of prograding beaches: A synthesis of seasonal- to century-scale observations of the Columbia River littoral cell. *Marine Geology*, 376, 51-68.